ChemPubSoc Europe

DOI: 10.1002/cphc.201500806

CHEMPHYSCHEM Communications

Investigation of DOTA–Metal Chelation Effects on the Chemical Shift of ^{129}Xe**

Keunhong Jeong,[a, b] Clancy C. Slack,[a, b] Christophoros C. Vassiliou,[a, b] Phuong Dao,[a, b] Muller D. Gomes,[a, b] Daniel J. Kennedy,[a, b] Ashley E. Truxal,[a, b] Lindsay J. Sperling,[d] Matthew B. Francis,[a, b] David E. Wemmer,[a, c] and Alexander Pines*[a, b]

Recent work has shown that xenon chemical shifts in cryptophane-cage sensors are affected when tethered chelators bind to metals. Here, we explore the xenon shifts in response to a wide range of metal ions binding to diastereomeric forms of 1,4,7,10-tetraazacyclododecane-1,4,7,10-tetraacetic acid (DOTA) linked to cryptophane-A. The shifts induced by the binding of Ca^{2+}, Cu^{2+}, Ce^{3+}, Zn^{2+}, Cd^{2+}, Ni^{2+}, Co^{2+}, Cr^{2+}, Fe^{3+}, and Hg^{2+} are distinct. In addition, the different responses of the diastereomers for the same metal ion indicate that shifts are affected by partial folding with a correlation between the expected coordination number of the metal in the DOTA complex and the chemical shift of ^{129}Xe. These sensors may be used to detect and quantify many important metal ions, and a better understanding of the basis for the induced shifts could enhance future designs.

Metal ions are very important in biological and environmental systems.[1] Some, including $Fe^{2/3+}$, Cu^{2+}, Co^{2+}, Zn^{2+}, and Ni^{2+}, play essential roles in human metabolism,[2] whereas others, including Hg^{2+}, Cd^{2+}, and Pb^{2+}, are toxic.[3] Although there are well-established methods for the in vitro detection of metals, including atomic absorption spectroscopy and various electrochemical techniques,[4] a practical technique that can simultaneously and nondestructively detect multiple metal ions would be a valuable addition to the existing analytical methods. Conventional NMR spectroscopy can distinguish between different chemical species, but is difficult to apply to complex mixtures. Although many metals have spin-active isotopes that can be detected by NMR spectroscopy, the sensitivity is generally very low. Here, we exploit the strong signals of hyperpolarized xenon, which are associated with a cryptophane cage carrying a metal chelator, to report the presence of metals through binding-induced shifts.

Hyperpolarized ^{129}Xe NMR/MRI has emerged as a promising in vivo imaging tool that is being explored extensively for the imaging of the lungs by using inspired xenon[5] and the study of brown fat and brain tissues by using dissolved xenon.[6] Additional work in vitro has established hyperpolarized ^{129}Xe NMR/MRI as a method for the selective, high-sensitivity detection of proteins,[7] enzyme activity,[8] nucleic acids,[9] and cell-surface receptors.[10] ^{129}Xe is useful as a reporter for a number of reasons: 1) There is no naturally occurring ^{129}Xe in the body, so there are no background signals that must be suppressed. 2) ^{129}Xe displays a large chemical shift in response to its physical and chemical surroundings, making it a sensitive reporter of the surrounding environment. 3) The ^{129}Xe NMR polarization is long-lived. Spin-exchange optical pumping of xenon can achieve almost complete polarization of the ^{129}Xe nuclei and allows the detection of low concentrations of ^{129}Xe dissolved in solution.[11]

Recent work by Zhang et al.[12] and Kotera et al.[13] developed cryptophane sensors that respond to Zn^{2+}, inducing a change in the chemical shift of the cryptophane-bound ^{129}Xe NMR peak upon metal binding. Changes in the chemical shifts were also observed upon binding Pb^{2+} and Cd^{2+} ions.[14] In the current work, we use the chelator 1,4,7,10-tetraazacyclododecane-1,4,7,10-tetraacetic acid (DOTA), which binds a wide range of metals with very high affinity, coupled to cryptophane-A and a solubilizing Glu_5 peptide (M0; Figure 1). We investigated a larger group of metals compared with previous work, including several that are paramagnetic. A comparison of the shifts

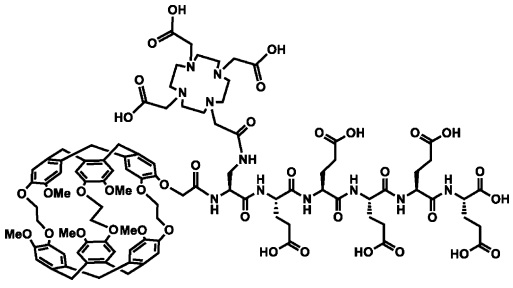

Figure 1. Sensor comprised of a cryptophane cage to bind xenon, a DOTA chelator, and solubilizing Glu_5 peptide (M0).

[a] K. Jeong, C. C. Slack, Dr. C. C. Vassiliou, P. Dao, M. D. Gomes, Dr. D. J. Kennedy, A. E. Truxal, Prof. Dr. M. B. Francis, Prof. Dr. D. E. Wemmer, Prof. Dr. A. Pines
Department of Chemistry, University of California
Berkeley, CA 94720-1460 (USA)
E-mail: pines@berkeley.edu

[b] K. Jeong, C. C. Slack, Dr. C. C. Vassiliou, P. Dao, M. D. Gomes, Dr. D. J. Kennedy, A. E. Truxal, Prof. Dr. M. B. Francis, Prof. Dr. A. Pines
Material Science Division, Lawrence Berkeley National Laboratory
Berkeley, CA 94720-1460 (USA)

[c] Prof. Dr. D. E. Wemmer
Physical Bioscience Division, Lawrence Berkeley National Laboratory
Berkeley CA 94720-1460 (USA)

[d] Dr. L. J. Sperling
Department of Chemistry and Biochemistry, Santa Clara University
Sata Clara, CA 95053-0270 (USA)

[**] DOTA = 1,4,7,10-tetraazacyclododecane-1,4,7,10-tetraacetic acid.

Supporting Information for this article is available on the WWW under http://dx.doi.org/10.1002/cphc.201500806.

induced by the different metals provides insight into the origin of the shifts, which may facilitate the design of improved multimetal sensors.

DOTA interacts strongly with transition-metal ions [log K_a = 22.2 (Cu^{2+}), 21.1 (Zn^{2+}), 21.3 (Cd^{2+}), 20.5 (Ni^{2+}), 20.3 (Co^{2+}), 16.4 (Ca^{2+}), 21.6 (Ce^{3+}), 24.4 (Fe^{3+}), and ≈23 (Hg^{2+}; from cyclam, estimated to have similar affinity with DOTA, due to its similar chemical structure)],[15] and essentially bind any free metals in a sample irreversibly. The affinity of metals for DOTA is stronger than most biological interactions, so, in a biological context, DOTA will act as a sink accumulating metals at a rate determined by their dissociation from the endogenous ligands.

DOTA is a flexible chelation agent with eight possible coordination points: four tertiary amines in the central ring and four carboxylate arms. The geometry of metal-bound DOTA is dependent on the specific metal present and its preferred coordination number (CN). Smaller metals prefer lower CN, for example six for Ga^{2+} (Figure 2).[16] Larger metals, for example

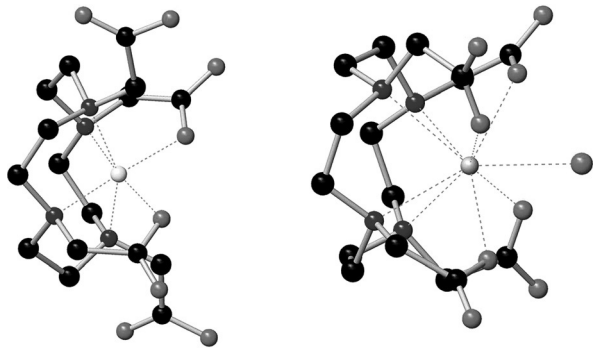

Figure 2. Crystallographically determined structures of DOTA bound to metal ions with coordination numbers of six, Ga^{2+} (left) and nine, Ce^{3+} (right).

those in the lanthanide series, favor high CNs using all eight ligand coordination points and incorporating a water molecule to give a CN of nine. The major geometries of interest are octahedral (CN = 6) and square antiprismatic (CN = 8).[15c] Metals bound with octahedral geometry (CN = 6) have two carboxylic acid arms unattached, which can interact with the cryptophane cage. Hyperpolarized ^{129}Xe in the cryptophane cage is positioned close to the metal ion, and even weak interactions between them can result in a distinct chemical shift, which depends upon the metal present. Cryptophane-A is intrinsically chiral, due to the handedness of the connection between the two cyclotriveratrylene units, and its synthesis yields an equal mix of the two enantiomers. When coupled to amino acids of pure chirality an equimolar mix of two diastereomers is created. For the current work, we used the mixture of the two, which turned out to be advantageous, because the metal-induced xenon shifts are different for each diastereomer.

We synthesized a water-soluble sensor minimizing the distance between DOTA and the cryptophane cage to increase the effect of metal binding on the chemical shift of xenon. The cryptophane cage is hydrophobic, and the solubility of DOTA decreases upon formation of a complex with a metal ion, so five glutamic acid residues were added to enhance solubility. The sensor was prepared by using solid-phase synthesis methods with a Wang resin. As a small linker between the cryptophane and DOTA, we added diaminopropionic acid in the last coupling before the addition of the cryptophane. The 1,4,7,10-tetraazacyclododecane-1,4,7,10-tetraacetic acid mono-*N*-hydroxysuccinimide (DOTA–NHS) ester was used to attach DOTA to the primary amine of aminoproprionate in an aqueous solution. The synthesized sensor was cleaved from the resin and purified with reversed-phase high-pressure liquid chromatography (HPLC). The synthesis route and structures are summarized in Figure 3.

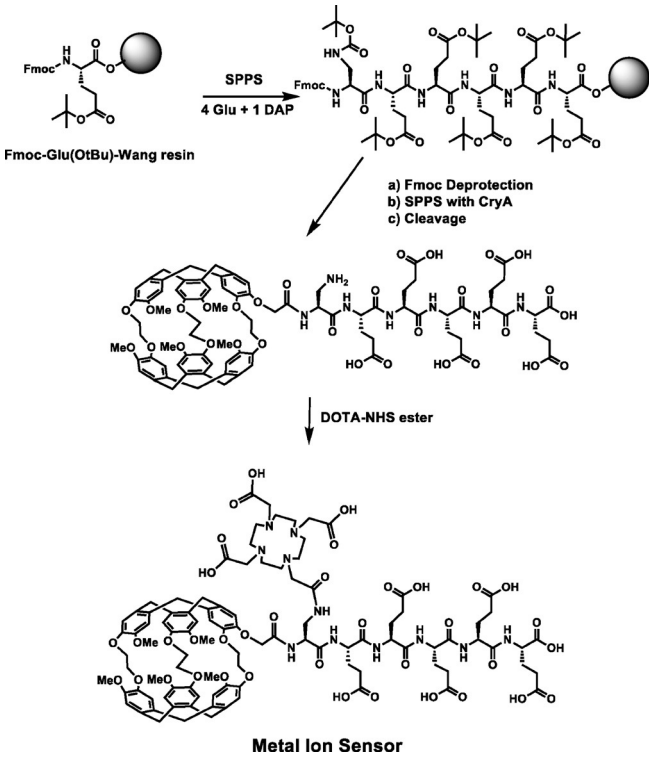

Figure 3. Synthesis of the metal-ion sensor. Five glutamic acid molecules, one diaminopropionic acid, and a cryptophane cage were attached to the Wang resin. They were then cleaved from the resin and DOTA was attached in aqueous solution.

The sensor was dissolved in phosphate buffer (pH 7.4) to give a solution with a concentration of 50 μM. Upon bubbling a polarized gas mixture containing ^{129}Xe (2% natural isotopic abundance Xe, 10% N_2, 88% He) into the solution, the two distinct peaks corresponding to the diastereomers of the structure were seen, as observed in previous work on diastereomeric sensors.[7c] Experiments were performed by adding a particular metal ion to a sensor solution in a 1:1 molar ratio. The solutions were then bubbled with the polarized gas mixture, and the dissolved ^{129}Xe NMR spectra were measured on a 9.4 T Varian NMR spectrometer.[17] As the chemical shift of ^{129}Xe is sensitive to temperature and pH,[18] all spectra were obtained under the same conditions (pH 7.4, 20 ± 0.1 °C). Each chemical shift was referenced to the dissolved ^{129}Xe signal.[12]

Changes in the chemical shift of xenon were determined upon the binding of the different metal ions, for example Cd^{2+} and Cu^{2+} (Figure 4). The induced changes in shift for a larger range of metals are shown in graphical format in Figure 5. It is

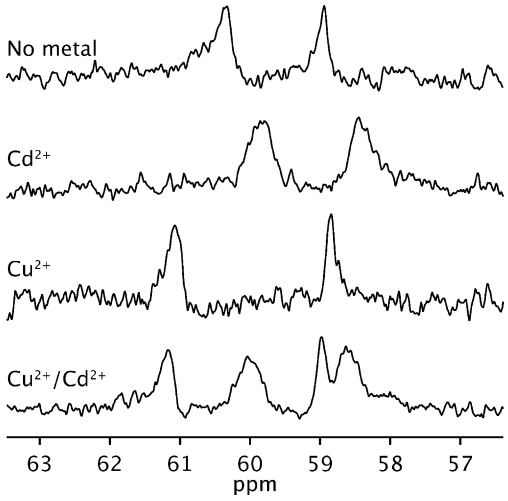

Figure 4. Comparison of ^{129}Xe spectra for 50 μM cryptophane complex with no metal, Cu^{2+}, Cd^{2+}, and a 50:50 mix of Cd^{2+} and Cu^{2+}.

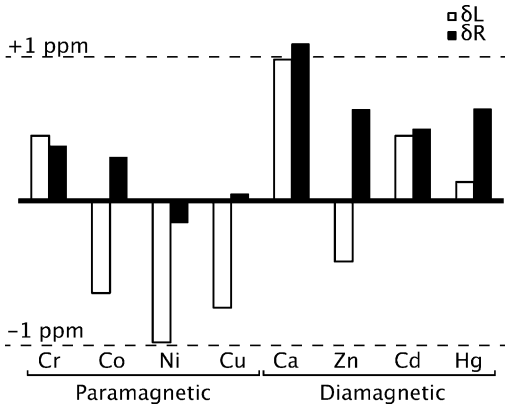

Figure 5. Comparison of the metal-induced xenon shift changes upon changing from the free sensor to the metal-bound sensor for each diastereomer. Metals are arranged from lowest to highest atomic number within each subset.

interesting to note that the metal-induced shift changes are different for the two diastereomers and distinct for each metal ion. These differences in shift are presumably associated with the way the peptide chain and DOTA moiety interact with the cryptophane cage through transient contacts. All of the ions featured in Figure 5 have a 2+ charge. There is no systematic pattern of change with atomic number or a consistent difference between paramagnetic and diamagnetic metals. The direction of the shift was most consistent for the diastereomers for which the free ligand is upfield of the bound ligand. The glutamate that resides in the solubilizing peptide can potentially interact with metals, so we also studied the cryptophane–peptide construct without the DOTA-chelating agent. The cryptophane cage with five glutamic acids attached was mixed with the same metal ions, but no ^{129}Xe NMR shifts were observed, thus supporting our view that the DOTA-bound metals induce the shift in the sensor and not the glutamate residues in the peptide. The distance between the bound metal and the xenon atom is large enough that paramagnetic relaxation does not dominate the xenon linewidth even with strongly relaxing metal ions, such as Ni^{2+}.

The first-row transition metals, Cr, Co, Ni, Cu, and Zn, form hexadentate complexes (CN = 6) with DOTA (all have an ionic radius between 0.69 and 0.74 Å). Metals with larger ionic radii, that is, Ca, Cd, and Hg (0.97–1.1 Å), form octadentate structures (CN = 8) with DOTA.[15c] Both diastereomers tend to have more upfield shifts within the CN = 8 complexes than the CN = 6 metals. Chemical-shift studies of even larger metals yielded multiple peaks as shown in Figure 6 for the sensor bound to

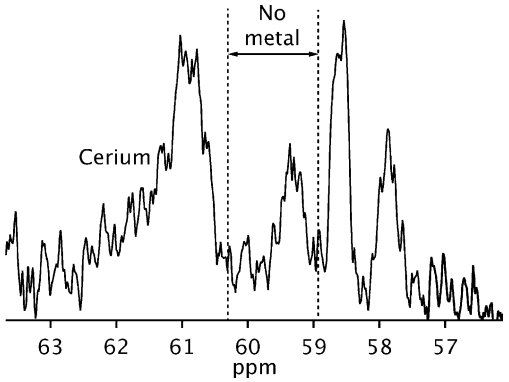

Figure 6. The ^{129}Xe spectrum of the cerium-bound sensor (CN = 9) shows four peaks versus two for the other metals, due to the two helical structures that the DOTA acetate arms form around the lanthanides. These two isomers are in slow exchange with each other giving rise to distinct peaks that are observable by using the sensor.

Ce^{3+}. Previous ^{1}H NMR studies of lanthanides bound to DOTA revealed a similar phenomenon where a slow exchange between different isomers of a capped square antiprismatic geometry (CN = 9) resulted in multiple peaks.[19] These two isomers represent the two helical structures that the acetate arms of the DOTA complex can take when bound to a metal ion, with an H_2O molecule acting as a cap on the complex. It has been previously shown that xenon detects differences in chirality;[7c] here this sensitivity can be exploited to observe the difference between isomeric pairs of metal complexes with the same coordination number.

The changes in chemical shift are modest for all metal ions ($\leq$1 ppm), but they are much larger than the observed linewidths making it possible to identify peaks for multiple metals in a single sample (Figure 4). Titrations of the sensor, starting with no metal ions and increasing to a 1:1 ratio with Fe^{3+} in increments of one quarter of the total concentration of M0, show resonances for the free and metal-bound forms in slow exchange (as expected from the high affinity of DOTA for all of the metals studied). The relative sizes of the resonances show that the intensities reflect the stoichiometry allowing for their

potential use in the quantitative determination of metal-ion concentrations (Figure 7). At 1:1 we have an equimolar ratio of Fe^{3+} to M0, which appears to correspond to less 100% bound

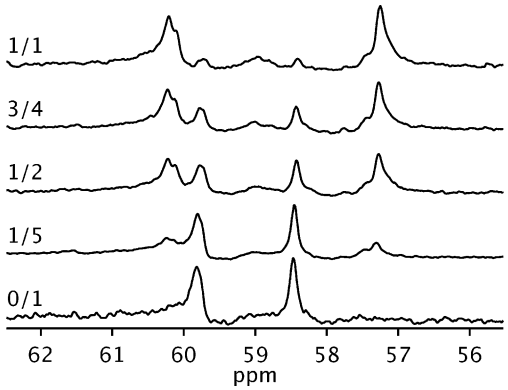

Figure 7. A series of spectra for the titration of Fe^{3+} into the sensor solution shows the simultaneous detection of the metal-bound and unbound sensor. The estimated ion-to-sensor ratio is shown alongside each spectrum, with 1/1 corresponding to approximately 95% bound.

due to a systematic error in the addition of Fe^{3+} to the sample. The variability of the metal-induced shifts indicates the challenge to optimize xenon-based metal-ion sensors to give maximal shift differences for distinct metals for the analysis of mixtures. Simulations performed by the Jameson group predict that the chemical shifts of a cryptophane-bound xenon atom are a function of the average distance from the methoxy groups on the surface of the cage, and hence, that shifts vary when contact causes a change in the shape of the cryptophane structure.[20] The high polarizability of xenon makes it very sensitive to its immediate environment, thus, very small changes owing to transient contacts can be detected. The binding of metal ions to the attached DOTA moiety causes distinct shifts for each diastereomer, which indicates that different interactions of the peptide/DOTA segment with the cage occur in the two diastereomers. A more complete understanding of the details may allow further optimization of the sensor for maximal response and its utility in metal analysis.

The signal-to-noise ratio in these experiments depends on the degree of polarization of the xenon and the fraction of ^{129}Xe in the gas. Increasing either of these would improve our ability to resolve the chemical-shift differences. Our experiments were performed with approximately 2% polarization of the natural isotope distribution of 26% ^{129}Xe. Using isotopically-enriched xenon and increasing the polarization would greatly increase the observed signal-to-noise ratio. Continuous-flow polarizers generating $>60\%$ polarization have been described,[21] and near-unity polarization has been achieved in batch processing polarizers.[22] In addition, the use of chemical exchange saturation transfer (CEST)[10] would provide further significant enhancement of the sensitivity. To maintain the resolution, optimization of the saturation power to avoid "power broadening" will be needed. Applying these approaches should make it possible to detect metal complexes in the low nanomolar concentration range. The ability to detect metals at low concentrations in the presence of more abundant ones will be determined by the separation between the xenon resonances of the particular species of interest. It has been shown that hyperpolarized xenon can be combined with MRI, and this combination makes it possible to image the spatial distribution of metals in a sample.[23]

Acknowledgements

This work was supported by the U.S. Department of Energy, Office of Science, Basic Energy Sciences, Materials Sciences, and Engineering Division, under Contract No. DE-AC02-05CH11231. K.J. acknowledges a fellowship from the Republic of Korea Army. C.C.S. acknowledges a graduate fellowship through the National Science Foundation.

Keywords: cryptophane · DOTA · metal-ion sensors · NMR spectroscopy · xenon

[1] D. T. Quang, J. S. Kim, *Chem. Rev.* **2010**, *110*, 6280 – 6301.
[2] Y. W. Choi, G. J. Park, Y. J. Na, H. Y. Jo, S. A. Lee, G. R. You, C. Kim, *Sens. Actuators B* **2014**, *194*, 343 – 352.
[3] E. Nieboer, D. H. Richardson, *Environ. Pollut. Ser. B* **1980**, *1*, 3 – 26.
[4] L. Cui, J. Wu, H. Ju, *Biosens. Bioelectron.* **2015**, *63*, 276 – 286.
[5] A.-M. Oros, N. J. Shah, *Phys. Med. Biol.* **2004**, *49*, R105.
[6] a) M. L. Mazzanti, R. P. Walvick, X. Zhou, Y. Sun, N. Shah, J. Mansour, J. Gereige, M. S. Albert, *PLoS One* **2011**, *6*, e21607; b) R. Xu, J. Ohya, L. Luo, *Segmentation of Brain MRI*, INTECH Open Access Publisher, **2012**. c) R. T. Branca, T. He, L. Zhang, C. S. Floyd, M. Freeman, C. White, A. Burant, *Proc. Natl. Acad. Sci. USA* **2014**, *111*, 18001 – 18006.
[7] a) A. Schlundt, W. Kilian, M. Beyermann, J. Sticht, S. Günther, S. Höpner, K. Falk, O. Roetzschke, L. Mitschang, C. Freund, *Angew. Chem. Int. Ed.* **2009**, *48*, 4142 – 4145; *Angew. Chem.* **2009**, *121*, 4206 – 4209; b) T. J. Lowery, S. Garcia, L. Chavez, E. J. Ruiz, T. Wu, T. Brotin, J. P. Dutasta, D. S. King, P. G. Schultz, A. Pines, *ChemBioChem* **2006**, *7*, 65 – 73; c) M. M. Spence, E. J. Ruiz, S. M. Rubin, T. J. Lowery, N. Winssinger, P. G. Schultz, D. E. Wemmer, A. Pines, *J. Am. Chem. Soc.* **2004**, *126*, 15287 – 15294.
[8] Q. Wei, G. K. Seward, P. A. Hill, B. Patton, I. E. Dimitrov, N. N. Kuzma, I. J. Dmochowski, *J. Am. Chem. Soc.* **2006**, *128*, 13274 – 13283.
[9] V. Roy, T. Brotin, J. P. Dutasta, M. H. Charles, T. Delair, F. Mallet, G. Huber, H. Desvaux, Y. Boulard, P. Berthault, *ChemPhysChem* **2007**, *8*, 2082 – 2085.
[10] L. Schröder, T. J. Lowery, C. Hilty, D. E. Wemmer, A. Pines, *Science* **2006**, *314*, 446 – 449.
[11] L. Schröder, *Physica Medica* **2013**, *29*, 3 – 16.
[12] J. Zhang, W. Jiang, Q. Luo, X. Zhang, Q. Guo, M. Liu, X. Zhou, *Talanta* **2014**, *122*, 101 – 105.
[13] N. Kotera, N. Tassali, E. Léonce, C. Boutin, P. Berthault, T. Brotin, J. P. Dutasta, L. Delacour, T. Traoré, D. A. Buisson, *Angew. Chem. Int. Ed.* **2012**, *51*, 4100 – 4103; *Angew. Chem.* **2012**, *124*, 4176 – 4179.
[14] N. Tassali, N. Kotera, C. L. Boutin, E. Léonce, Y. Boulard, B. Rousseau, E. Dubost, F. d. r. Taran, T. Brotin, J.-P. Dutasta, *Anal. Chem.* **2014**, *86*, 1783 – 1788.
[15] a) H. Maumela, R. D. Hancock, L. Carlton, J. H. Reibenspies, K. P. Wainwright, *J. Am. Chem. Soc.* **1995**, *117*, 6698 – 6707; b) E. L. Que, D. W. Domaille, C. J. Chang, *Chem. Rev.* **2008**, *108*, 1517 – 1549; c) N. Viola-Villegas, R. P. Doyle, *Coord. Chem. Rev.* **2009**, *253*, 1906 – 1925.
[16] a) A. Heppeler, J. P. André, I. Buschmann, X. Wang, J. C. Reubi, M. Hennig, T. A. Kaden, H. R. Maecke, *Chem. Eur. J.* **2008**, *14*, 3026 – 3034; b) F. Benetollo, G. Bombieri, L. Calabi, S. Aime, M. Botta, *Inorg. Chem.* **2003**, *42*, 148 – 157.
[17] K. K. Palaniappan, R. M. Ramirez, V. S. Bajaj, D. E. Wemmer, A. Pines, M. B. Francis, *Angew. Chem. Int. Ed.* **2013**, *52*, 4849 – 4853; *Angew. Chem.* **2013**, *125*, 4949 – 4953.

[18] C. Witte, L. Schröder, *NMR Biomed.* **2013**, *26*, 788 – 802.
[19] S. Aime, M. Botta, M. Fasano, M. P. M. Marques, C. F. Geraldes, D. Pubanz, A. E. Merbach, *Inorg. Chem.* **1997**, *36*, 2059 – 2068.
[20] a) D. N. Sears, C. J. Jameson, *J. Chem. Phys.* **2003**, *119*, 12231 – 12244; b) E. J. Ruiz, D. N. Sears, A. Pines, C. J. Jameson, *J. Am. Chem. Soc.* **2006**, *128*, 16980 – 16988.
[21] I. Ruset, S. Ketel, F. Hersman, *Phys. Rev. Lett.* **2006**, *96*, 053002.
[22] P. Nikolaou, A. M. Coffey, L. L. Walkup, B. M. Gust, N. Whiting, H. Newton, S. Barcus, I. Muradyan, M. Dabaghyan, G. D. Moroz, M. S. Rosen, S. Patz, M. J. Barlow, E. Y. Chekmenev, B. M. Goodson, *Proc. Natl. Acad. Sci. USA* **2013**, *110*, 14150 – 14155.
[23] B. Driehuys, J. Pollaro, G. P. Cofer, *Magn. Reson. Med.* **2008**, *60*, 14 – 20.

Manuscript received: September 14, 2015
Accepted Article published: September 17, 2015
Final Article published: October 7, 2015